Monthly Notices of the ROYAL ASTRONOMICAL SOCIETY
MNRAS **450,** L11–L15 (2015) doi:10.1093/mnrasl/slv036

Wind-induced odd gravitational harmonics of Jupiter

Dali Kong,[1] Keke Zhang[2★] and Gerald Schubert[3]

[1] *Key Laboratory of Planetary Sciences, Shanghai Astronomical Observatory, Chinese Academy of Sciences, Shanghai 200030, China*
[2] *Center for Geophysical and Astrophysical Fluid Dynamics, University of Exeter, Exeter EX4 4QF, UK*
[3] *Department of Earth, Planetary and Space Sciences, University of California, Los Angeles, CA 90095-1567, USA*

Accepted 2015 February 26. Received 2015 February 25; in original form 2015 January 6

ABSTRACT

While the rotational distortion of Jupiter makes a major contribution to its lowermost order even zonal gravitational coefficients J_n with $n \geq 2$, the component of the zonal winds with equatorial antisymmetry, if sufficiently deep, produces a gravitational signature contained in the odd zonal gravitational coefficients J_n with $n \geq 3$. Based on a non-spherical model of a polytropic Jupiter with index unity, we compute Jupiter's odd gravitational coefficients J_3, J_5, $J_7, \ldots, J_{11}$ induced by the equatorially antisymmetric zonal winds that are assumed to be deep. It is found that the lowermost odd gravitational coefficients J_3, J_5 and J_7 are of the same order of magnitude with $J_3 = -1.6562 \times 10^{-6}$, $J_5 = 1.5778 \times 10^{-6}$ and $J_7 = -0.7432 \times 10^{-6}$, and are within the accuracy of high-precision gravitational measurements to be carried out by the *Juno* spacecraft.

Key words: planets and satellites: atmospheres – planets and satellites: interiors.

1 INTRODUCTION

Jupiter is rotating rapidly, resulting in significant departure from spherical geometry: its shape eccentricity at the one-bar surface is $\mathcal{E}_{\rm J} = 0.3543$ (Seidelmann et al. 2007). The shape and gravitational field of Jupiter can provide an important constraint on the physical and chemical properties of its interior. In 2016, the *Juno* spacecraft, now on its way to Jupiter, will make high-precision measurements of the Jovian gravitational field (Hubbard 1999; Bolton 2005) whose zonal external potential $V_{\rm g}$ can be expanded in terms of the Legendre functions P_n,

$$V_{\rm g} = -\frac{GM_{\rm J}}{r}\left[1 - \sum_{n=2}^{\infty} J_n \left(\frac{R_{\rm e}}{r}\right)^n P_n(\cos\theta)\right], \quad r \geq R_{\rm e}, \qquad (1)$$

where $M_{\rm J}$ is Jupiter's mass, n takes integer values, J_2, J_3, J_4, J_5, …, are the zonal gravitational coefficients, (r, θ, ϕ) are spherical polar coordinates with the corresponding unit vectors $(\hat{\boldsymbol{r}}, \hat{\boldsymbol{\theta}}, \hat{\boldsymbol{\phi}})$ and $\theta = 0$ is the axis of rotation, $R_{\rm e}$ is the equatorial radius of Jupiter and G is the universal gravitational constant ($G = 6.673\,84 \times 10^{-11}$ m^3 kg^{-1} s^{-2}). At present, only the first three even zonal gravitational coefficients J_2, J_4, J_6, which are mainly produced by the effect of rotational distortion of Jupiter, are accurately measured. By circling Jupiter in a polar orbit, the *Juno* spacecraft will carry out high-precision measurements of the gravitational coefficients up to J_{12} (Bolton 2005). While both the rotational distortion and the equatorially symmetric zonal winds contribute to the even gravitational coefficients J_n with $n \geq 2$, the component of the equatorially antisymmetric winds, if sufficiently deep, induces the odd coefficients J_n with $n \geq 3$. How the equatorially symmetric zonal winds modify the even gravitational coefficients J_n with $n \geq 2$ has been investigated in several studies (Hubbard 1999; Kaspi et al. 2010; Kong et al. 2013). This study focuses on the odd gravitational coefficients J_n with $n \geq 3$ in equation (1) caused by the equatorially antisymmetric zonal winds that are assumed to be deep.

In a recent study, Kong et al. (2014) computed the gravitational signature produced by the Jovian equatorial winds that are equatorially symmetric and confined within a small equatorial region between the latitudes $\varphi = \pm 25^\circ$ with the maximum penetration depth about 10 per cent of Jupiter's equatorial radius containing about 0.18 per cent of the total Jovian mass. The study was motivated by the likelihood that the equatorial zonal jets cannot be strongly affected by either the Jovian magnetic field or the stable stratification (Liu, Goldreich, & Stevenson 2008; Lian & Showman 2010; Gastine & Wicht 2012). By comparing to the results from a model of the deep zonal winds at all latitudes, Kong et al. (2014) found the equatorial zonal jets contribute 90 per cent of the high-order even gravitational coefficient J_{12} in equation (1). Thus, the high-order gravitational coefficients – whose values were thought to reflect the penetration depth of the zonal winds – are nearly independent of the depth of the Jovian zonal winds in the non-equatorial regions with the latitudes $25^\circ \leq \varphi \leq 90^\circ$ and $-90^\circ \leq \varphi \leq -25^\circ$. This result highlights the importance of the gravitational signature contained in the odd gravitational coefficients in equation (1) produced by the component of the equatorially antisymmetric zonal winds.

It is important to notice that, while the effect of Jupiter's departure from spherical geometry makes a leading-order contribution to the lower-order even gravitational coefficients J_n with

★ E-mail: kzhang@ex.ac.uk

$n \geq 2$ in equation (1), the non-spherical effect is likely less significant on estimating the lower-order odd gravitational coefficients J_n with $n \geq 3$ caused by the equatorially antisymmetric zonal winds. Kaspi (2013) carried out the first study of the gravitational signature induced by the equatorially antisymmetric zonal winds in Jupiter which rotates with the angular velocity $\boldsymbol{\Omega}$ and is assumed to be spherical. He considered the thermal wind equation in the form

$$-2\boldsymbol{\Omega} \cdot \nabla(\rho_0 \boldsymbol{u}) = \nabla \rho' \times \boldsymbol{g}_0, \tag{2}$$

where ρ_0 and $\boldsymbol{g}_0$ represent the density and gravity profile of the hydrostatic state, respectively, while ρ' denotes the density perturbation to ρ_0 caused by the zonal winds $\boldsymbol{u}$. Upon neglecting the effect of non-spherical geometry, $\boldsymbol{g}_0$ is only a function of r and can be readily related to the density profile $\rho_0(r)$ from an interior model (see, for example, Guillot & Morel 1995). By denoting the zonal winds $\boldsymbol{u} = U(r, \theta)\hat{\boldsymbol{\phi}}$, the azimuthal component of equation (2) gives rise to the density perturbation

$$\rho'(r, \theta) = C(r) + \frac{2r\Omega}{|\boldsymbol{g}_0(r)|} \times \int_{\pi/2}^{\theta} \left[\cos\theta \frac{\partial}{\partial r}(\rho_0 U) + \frac{\sin\theta}{r}\frac{\partial}{\partial \theta}(\rho_0 U)\right] \mathrm{d}\theta, \tag{3}$$

where $C(r)$ is an arbitrary function of r. Kaspi (2013) recognized that

$$\int_0^{\pi}\int_0^{R} C(r) P_{2l+1}(\cos\theta)\, r^2 \sin\theta \,\mathrm{d}r\,\mathrm{d}\theta = 0, \quad l = 1, 2, 3, \ldots,$$

where R is the radius of a spherical planet. It follows that the arbitrary function $C(r)$ does not make any contribution to the odd gravitational coefficients J_n in equation (1). By performing the integration over θ in equation (3) using a given $\rho_0(r)$ and $\boldsymbol{g}_0(r)$ together with

$$U(r, \theta) = u_0(r, \theta)\mathrm{e}^{-(R-r)/H}, \tag{4}$$

where $u_0(r = R, \theta)$ denotes the observed cloud-level zonal winds which extend into the interior on cylinders parallel to the rotation axis and H is a depth parameter, Kaspi (2013) calculated the values of $J_3, J_5, J_7, \ldots$ in equation (1) for different values of H. When H becomes sufficiently large, the values of $J_3, J_5, J_7, \ldots$ represent an upper bound on the odd zonal gravitational coefficients in equation (1). This approach based on equation (3) is inapplicable to rapidly rotating giant gaseous planets that depart substantially from spherical geometry.

In this study, we compute the odd gravitational coefficients J_n with $n = J_3, J_5, \ldots, J_{11}$ in equation (1) induced by the component of the equatorially antisymmetric zonal winds in the rotationally distorted, non-spherical Jupiter without making use of the thermal wind equation (2). The non-spherical geometry represents a mathematically difficult and challenging problem because the spherical-harmonic-expansion method – which can treat the equatorial symmetry by simply selecting different parities in the spherical harmonic expansion – is no longer suitable. We carry out an accurate computation of the gravitational coefficients $J_3, J_5, J_7, \ldots, J_{11}$ in equation (1) for the oblate spheroidal Jupiter with its shape eccentricity $\mathcal{E}_\mathrm{J} = 0.3543$ using a three-dimensional finite- element mesh containing 32×10^6 tetrahedral elements. An unusual mathematical approach has to be adopted in order to capture the equatorial antisymmetry when using a fully three-dimensional finite-element method. Instead of solving the governing equations in the whole oblate spheroidal domain of Jupiter, we solve them in the Northern hemisphere of Jupiter such that the equatorially antisymmetric condition required at the equatorial plane can be explicitly imposed. In comparison to the approach based on the thermal wind equation (2) in spherical geometry (Kaspi 2013), our approach is geometrically non-spherical as is the rapidly rotating Jupiter and mathematically marked by the uniqueness of the solution satisfying an appropriate physical boundary condition. We begin by presenting the model and the governing equations in Section 2 which is followed by the discussion of the results in Section 3 while a summary and some remarks are given in Section 4.

2 MODEL AND GOVERNING EQUATIONS

Our model assumes that (i) Jupiter with mass M_J and equatorial radius R_e is isolated and rotating rapidly about the symmetry z-axis with an angular velocity $\Omega\hat{\boldsymbol{z}}$, (ii) Jupiter is axially symmetric, described by an oblate spheroid with eccentricity $\mathcal{E}_\mathrm{J} = 0.3543$ (Seidelmann et al. 2007), and consists of a compressible barotropic fluid (a polytrope of index unity) whose density ρ is a function only of the pressure p (Chandrasekhar 1933; Roberts 1962; Hubbard 1999) and (iii) the zonal winds observed on Jupiter have an equatorially antisymmetric component that depends only on distance s from the rotation axis and extends from the cloud surface to the equatorial plane. In an inertial frame of reference, the equilibrium equations are

$$\boldsymbol{u} \cdot \nabla \boldsymbol{u} = -\frac{1}{\rho}\nabla p - \nabla V_\mathrm{g}, \tag{5}$$

$$\nabla^2 V_\mathrm{g} = 4\pi G \rho, \tag{6}$$

$$\nabla \cdot (\boldsymbol{u}\rho) = 0, \tag{7}$$

where $\boldsymbol{u}$ denotes the fluid motion and V_g represents the gravitational potential. Equations (5)–(7) are solved subject to the two boundary conditions

$$p = 0, \tag{8}$$

$$V_\mathrm{g} + V_\mathrm{c} = \text{constant}, \tag{9}$$

at the bounding surface $\mathcal{S}$ of Jupiter described by $r = \widetilde{R}(\theta)$, where V_c is the centrifugal potential.

We solve equations (5)–(7) by making the expansions

$$\rho = \rho_0 + \rho_1, \quad p = p_0 + p_1, \quad \boldsymbol{u} = \Omega\hat{\boldsymbol{z}} \times \boldsymbol{r} + U(r, \theta)\hat{\boldsymbol{\phi}}, \tag{10}$$

where $U(r, \theta)\hat{\boldsymbol{\phi}}$ denotes the profile of the zonal winds satisfying

$$\frac{U_0}{\Omega R_\mathrm{e}} \ll 1,$$

where U_0 is the typical speed of the winds. In the leading-order problem, we determine the bounding surface $r = \widetilde{R}(\theta)$ and compute the even zonal gravitational coefficients J_2, J_4, J_6 up to J_{12} taking into account the full rotational distortion (Kong et al. 2013). In the next-order problem, which is the focus of this study, we compute the odd zonal gravitational coefficients J_3, J_5, J_7 up to J_{11} in the expansion (1) induced by the deep equatorially antisymmetric winds $U(r, \theta)$ that satisfy

$$U(r, \theta) = -U(r, \pi - \theta) \quad \text{for} \quad 0 < \theta < \pi/2, \tag{11}$$

where $U(r = \widetilde{R}(\theta), \theta)$ at the bounding surface of Jupiter represents the observed, equatorially antisymmetric cloud-level zonal winds.

It is important to notice that the equatorially antisymmetric winds only produce the density anomaly ρ_1 that is also equatorially antisymmetric, imposing the extra boundary condition

$$\rho_1(r, \theta = \pi/2) = 0 \text{ at the equatorial plane.} \quad (12)$$

In the rotationally distorted Jupiter whose shape is described by $r = \widetilde{R}(\theta)$, the equatorially antisymmetric condition (12) has to be explicitly imposed using an appropriate numerical method.

3 METHOD AND RESULTS

The observed Jovian winds (Porco et al. 2003) can be decomposed into two different components: the equatorially symmetric winds and the equatorially antisymmetric winds. Fig. 1 shows the profile of the total observed Jovian cloud-level zonal winds and its decomposition. The strength of the equatorially antisymmetric component is weaker than that of the symmetric component. We assume that the equatorially antisymmetric zonal winds shown in Fig. 1(c) extend on cylinders parallel to the axis of rotation from the cloud level to the equatorial plane, which represents the case of the profile given by equation (4) with sufficiently large H.

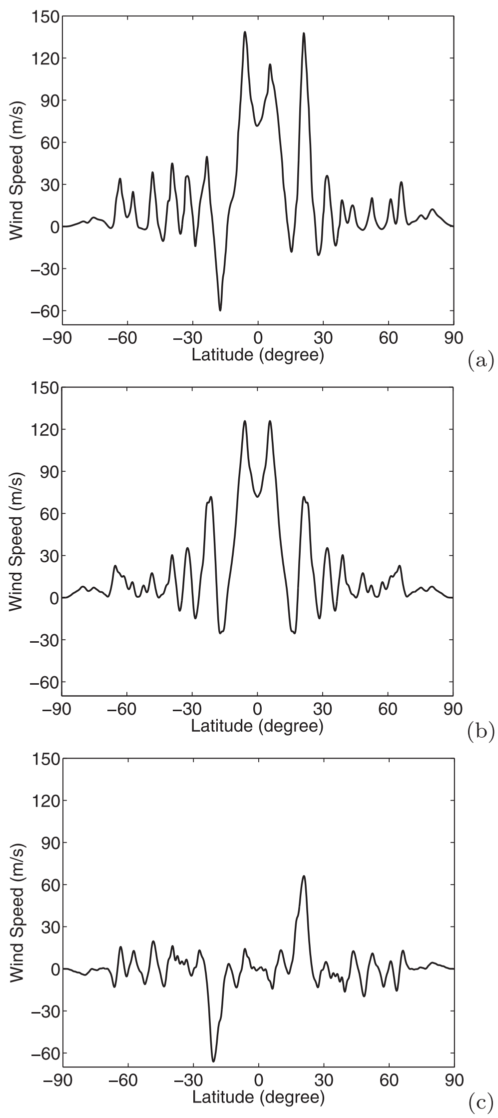

Figure 1. (a) The profile of the total observed Jovian zonal winds at the cloud level, (b) the profile of its equatorially symmetric component and (c) the profile of its equatorially antisymmetric component.

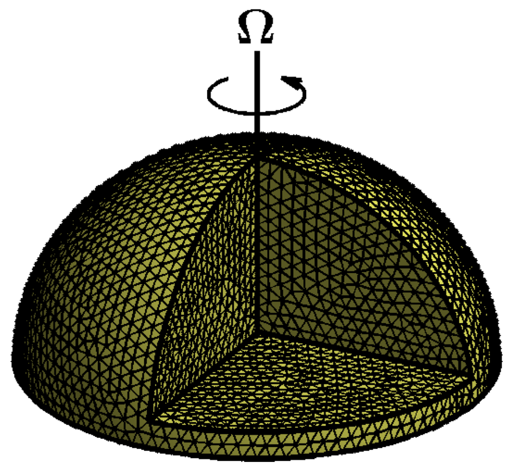

Figure 2. Sketch of a three-dimensional tetrahedral mesh in the Northern hemisphere which also represents the domain of the numerical solution in this Letter. At the equatorial plane, the density anomaly ρ_1 induced by the equatorially antisymmetric zonal winds must vanish. In our actual numerical computation, 32×10^6 tetrahedral elements in the Northern hemisphere are used for the numerical computation.

It should be emphasized that the equatorially antisymmetric winds $U(r, \theta)$ defined by equation (11) and shown in Fig. 1(c) induce the density anomaly ρ_1 obeying the parity,

$$\rho_1(r, \theta) = -\rho_1(r, \pi - \theta),$$

which produces only the odd gravitational coefficients J_n with $n \geq 3$. A challenging numerical hurdle is how to enforce the equatorially antisymmetric condition (12) in a non-spherical planet when using a three-dimensional, local numerical method. We found that an effective way of computing an antisymmetric solution satisfying equation (12) is to solve only the Northern hemisphere of the planet defined by $0 \leq \theta < \pi/2$ and $0 \leq r < \widetilde{R}(\theta)$ such that both the boundary conditions at $r = \widetilde{R}(\theta)$ given by equation (8) and at $\theta = \pi/2$ given by equation (12) can be explicitly imposed. The solution of the Southern hemisphere defined by $\pi/2 < \theta \leq \pi$ and $0 \leq r < \widetilde{R}(\theta)$ can be simply obtained by making use of the symmetry property.

A three-dimensional finite-element method – whose high accuracy in non-spherical geometry was confirmed by an exact solution (Kong, Zhang & Schubert 2015) – is employed to solve equations (5)–(7) for the density anomaly ρ_1 satisfying the conditions (8) and (12). We construct a three-dimensional finite-element mesh by making a tetrahedralization of the Northern hemisphere of Jupiter with its shape eccentricity $\mathcal{E} = 0.3543$. A sketch of the finite-element mesh for the northern spheroidal domain is illustrated in Fig. 2, which contains 0.16×10^6 tetrahedral elements. In comparison to a spectral method, our finite-element method is local, free of the pole and central numerical singularities and, more significantly, geometrically flexible. A Galerkin weighted residual approach is adopted in the finite-element formulation along with a Krylov subspace iterative method. For the results reported in this Letter, the northern spheroidal domain is divided into about 32×10^6 tetrahedral elements that enable us to compute the accurate odd gravitational coefficients up to J_{11}. All the numerical computations presented in this Letter are fully three-dimensional, but all the numerical solutions turn out to be always axisymmetric.

Fig. 3 shows the meridional cross-section of the density anomaly ρ_1 in the northern interior of Jupiter, reflecting the redistribution of

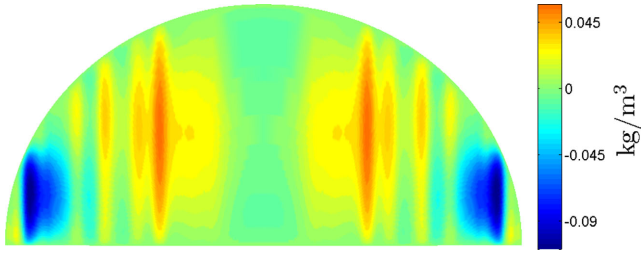

Figure 3. The equatorially antisymmetric density anomaly ρ_1 in a meridional plane of the Northern hemisphere induced by the equatorially antisymmetric deep winds.

Table 1. The odd zonal gravitational coefficients J_n, $n \geq 3$ in the expansion (1) induced by the equatorially antisymmetric zonal winds in the rotationally distorted Jupiter.

n	$J_n \times 10^6$
3	– 1.6562
5	1.5778
7	– 0.7432
9	0.3168
11	– 0.0210

mass within Jupiter due to the effect of the deep equatorially antisymmetric zonal winds depicted in Fig. 1(c). The density anomaly ρ_1 takes place largely within the cylindrical structure in the interior region where the zonal winds are strong. In the vicinity of $r = \widetilde{R}(\theta)$ and $\theta = \pi/2$ where the boundary condition (8) and the symmetry condition (12) must be satisfied, however, the density anomaly ρ_1 is weak. After obtaining the density anomaly ρ_1, we can then compute the odd zonal gravitational zonal coefficients J_n with $n \geq 3$, induced by the deep winds in equation (11), by performing the two-dimensional integration over the non-spherical Jupiter

$$J_n = -\frac{4\pi}{M_{\rm J} R_{\rm e}^n} \times \int_0^{\pi/2} \int_0^{\widetilde{R}(\theta)} \rho'(r,\theta) P_n(\theta) \sin\theta \, r^{n+2} \, {\rm d}r \, {\rm d}\theta, \qquad (13)$$

for $n = 3, 5, 7, \ldots, 11$. The results are presented in Table 1, showing that the effect of the zonal winds yields the strongest gravitational signature in the lowermost order odd coefficients J_3, J_5 and J_7 which are of the same order of magnitude. For instance, $|J_3| = 1.6562 \times 10^{-6}$ is of the same order as $|J_7| = 0.7432 \times 10^{-6}$. They represent an upper bound on the odd gravitational coefficients that can be induced by the equatorially antisymmetric zonal winds on the rotationally distorted Jupiter. More significantly, the size of the odd coefficients J_3, J_5 and J_7 is well within the accuracy of the high-precision gravity measurements to be carried out the *Juno* spacecraft in 2016 (Bolton 2005).

4 SUMMARY AND REMARKS

The Jovian zonal winds have been accurately measured and extensively studied for a number of decades, but their generation and penetration depth still remain highly controversial (Ingersoll & Cuzzi 1969; Busse 1976; Zhang & Schubert 1996; Liu et al. 2008; Jones & Kunzanyan 2009; Lian & Showman 2010; Gastine & Wicht 2012). An important objective of the *Juno* spacecraft is to probe the extent of penetration of the zonal winds into the interior of Jupiter by accurately measuring their effects on its gravitational field with unprecedentedly high precision. Since the high-order coefficients J_n with even n are found to be nearly independent of the depth of the zonal winds in the non-equatorial regions (Kong et al. 2014), and since the size of J_n with odd n are directly related to the depth of the equatorially antisymmetric zonal winds (Kaspi 2013), accurately determining the odd coefficients J_n in equation (1) would play a critical role in understanding the structure of the zonal winds in the deep interior of Jupiter.

This study, based on the polytropic model of Jupiter with index unity (Chandrasekhar 1933; Hubbard 1999), represents an attempt to compute the odd gravitational coefficients, $J_3, J_4, \ldots, J_{11}$, induced by the equatorially antisymmetric zonal winds in a rotationally distorted gaseous Jupiter. In order to impose the equatorially antisymmetric condition (12) at the equatorial plane, we have constructed a three-dimensional finite-element mesh by making a tetrahedralization of the Northern hemisphere of Jupiter and, then, solving the governing equations in the Northern hemisphere. The solution for the Southern hemisphere is obtained simply by using the equatorial antisymmetry. It is found that the lowermost-order odd coefficients J_3, J_5 and J_7 – which correspond to the case with the profile given by equation (4) for sufficiently large H – are of the same order of magnitude $O(10^{-6})$.

Our results are, however, substantially different from those of the previous study (Kaspi 2013) in spherical geometry based on the thermal wind equation (2). In the fig. 4 of Kaspi (2013), the values of the odd coefficients J_3, J_5 and J_7 are displayed as a function of H for $10\,{\rm km} \leq H \leq 6 \times 10^4\,{\rm km}$ in which J_3, J_5 and J_7 show an asymptotic behaviour when $H > 2 \times 10^4$ km. It follows that a direct comparison can be made between our results and those of Kaspi (2013) when H in equation (4) is sufficiently large. The values of the odd coefficients J_3, J_5 and J_7 from his spherical model can be estimated from the fig. 4 of Kaspi (2013). In particular, Kaspi (2013) obtained $J_7 \approx 6 \times 10^{-7}$ for large H, while our computation gives $J_7 = -7.4 \times 10^{-7}$. There is also an O(100) per cent difference in the size of J_3: his value is $J_3 \approx -10^{-6}$ while our computation yields $J_3 = -1.66 \times 10^{-6}$. Although his value for J_5 does not fully reach the asymptotic value for large H in his fig. 4, it also indicates a more than 100 per cent difference: his value is $J_5 \approx 0.4 \times 10^{-6}$ while ours is $J_5 = 1.58 \times 10^{-6}$.

It should be recognized that there exist several significant differences between our model and that of Kaspi (2013). First, our model has non-spherical geometry while his is spherical. However, it is anticipated that the effect of geometry would not cause a substantial difference in the values of odd gravitational coefficients. Secondly, our model is mathematically marked by a solution of equations (5)–(7) satisfying the boundary condition (8) required at the bounding surface $r = \widetilde{R}(\theta)$ while his model is based on the thermal wind equation (2) that represents a diagnostic relation and does not require any boundary condition. Thirdly, our model has assumed that the compressible fluid in Jupiter is barotropic and, hence, the zonal winds U must satisfy the geostrophic condition, i.e. $\partial U/\partial z = 0$, where z denotes the coordinate in the direction of rotation axis, while Kaspi (2013) did not make the barotropic assumption – which represents an important advantage of his spherical model. The profile of the equatorially antisymmetric zonal winds U in our model satisfies the geostrophic condition $\partial U/\partial z = 0$ everywhere in both the Northern hemisphere defined by $0 \leq \theta < \pi/2$ and $0 \leq r \leq \widetilde{R}(\theta)$ and the Southern hemisphere defined by $\pi/2 < \theta \leq \pi$ and $0 \leq r \leq \widetilde{R}(\theta)$. But it introduces a physically unrealistic shear at the equatorial plane $\theta = \pi/2$ – which represents a disadvantage of our non-spherical model. Since the wind-induced density anomaly ρ_1 vanishes exactly at the equatorial plane $\theta = \pi/2$ in the form of the imposed boundary condition, it is expected that the shear at $\theta = \pi/2$ would produce insignificant effects on the odd gravitational coefficients. Evidently, a further study is required to identify the key reasons why there exist such large differences between our results and those of Kaspi (2013).

ACKNOWLEDGEMENTS

DK is supported by the NSFC under grant 11473014, KZ is supported by the UK STFC under grant ST/J001627/1 and the HKRGC grant (Project 14306814), and GS is supported by the National Science Foundation under grant NSF AST-0909206. The computation made use of the high performance computing resources in the Core Facility for Advanced Research Computing at Shanghai Astronomical Observatory, Chinese Academy of Sciences.

REFERENCES

Bolton S. J., 2005, Tech. Rep. AO-03-OSS-03, Juno Final Concept Study Report. NASA, Washington, DC
Busse F., 1976, Icarus, 29, 255
Chandrasekhar S., 1933, MNRAS, 93, 390
Gastine T., Wicht J., 2012, Icarus, 219, 428
Guillot T., Morel P., 1995, A&AS, 109, 109
Hubbard W. B., 1999, Icarus, 137, 357
Ingersoll A. P., Cuzzi J. N., 1969, J. Atmos. Sci., 26, 981
Jones C. A., Kuzanyan K. M., 2009, Icarus, 204, 227
Kaspi Y., 2013, Geophys. Res. Lett., 40, 676
Kaspi Y., Hubbard W. B., Showman A. P., Flierl G. R., 2010, Geophys. Res. Lett., 37, L01204
Kong D., Liao X., Zhang K., Schubert G., 2013, Icarus, 226, 1425
Kong D., Liao X., Zhang K., Schubert G., 2014, ApJ, 791, L24
Kong D., Zhang K., Schubert G., 2015, MNRAS, 448, 456
Lian Y., Showman A. P., 2010, Icarus, 207, 373
Liu J., Goldreich P. M., Stevenson D. J., 2008, Icarus, 196, 653
Porco C. C. et al., 2003, Science, 299, 1541
Roberts I. P. H., 1962, ApJ, 136, 1108
Seidelmann P. K. et al., 2007, Celest. Mech. Dyn. Astron., 98, 155
Zhang K., Schubert G., 1996, Science, 273, 941